Scientia Iranica C (2015) 22(6), 2309–2318

SCIENTIA IRANICA

Sharif University of Technology
Scientia Iranica
Transactions C: Chemistry and Chemical Engineering
www.scientiairanica.com

Enantioselectivity of lipase B from *Candida antarctica* in the transesterification reaction of (*R*, *S*)-1-phenylethanol and *S*-ethyl thio-octanoate; a density functional study

M. Irani* **and S. Heydaryan**

Department of Chemistry, University of Kurdistan, Sanandaj, P.O. Box 66177-15177, Iran.

Received 14 September 2014; received in revised form 19 December 2014; accepted 25 April 2015

KEYWORDS
Lipase B;
DFT;
Quantum cluster;
Enantioselectivity;
Transesterification.

Abstract. The catalyzed reaction of *(R,S)*-1-phenylethanol and *S*-ethyl thio-octanoate by lipase B from *Candida antarctica* is studied using density functional theory. Quantum mechanics cluster approach is used to model the enzyme's active site. The results show that the catalytic triad amino acids of the enzyme do not abstract the alcoholic proton of 1-phenylethanol before a nucleophilic attack from the alcohol to the ester. A two-step mechanism is proposed for the reaction of *R*-enantiomer of the alcohol with the ester. However, the results show no path for the *S*-enantiomer. We showed that enantioselectivity of the enzyme is due to different hydrogen-bonding patterns of the two enantiomers of the alcohol in the enzyme's active site. The OH group of *R*-enantiomer is directed toward Ser-105, while the OH group of *S*-enantiomer is far from Ser-105 and is directed toward Thr-40.

1. Introduction

Enzymes are macromolecules which play a vital role in catalyzing chemical reactions inside living cells. The rate of most biochemical reactions would be very slower than the required rate for proceeding life processes. They are biocatalysts which support almost all kinds of chemical reactions. Enzymes have special characteristics such as stereoselectivity and enantioselectivity. These unique properties make them an important subject for experimental and theoretical studies.

Lipases are a big family of enzymes which catalyze the breakdown or hydrolysis of fats. They are a subclass of esterases and perform essential roles in digestion, transportation, and processing of dietary lipids in most living organisms. In addition, lipases are of general interest within many industrial applications. They are used within the industries, e.g. detergents, oil and fats, baking, organic synthesis, hard surface cleaning, leather industry, and paper industry [1-5].

Many lipases contain one or more α-helixes, which form a lid. These lipases are usually inactive when this lid covers the active site. When a lipase approaches a hydrophobic surface, the lid uncovers the active site, exposing it to the substrate and making it active [6,7]. Lipases are usually active not only at a water/hydrophobic interface but also in organic solvents [8]. They are surprisingly flexible biocatalysts for the acylation or deacylation of a wide range of unnatural substrates.

Lipase B from *Candida antarctica* (CalB) is one of the most widely used biocatalysts in industry [3]. CalB has a molecular mass of 33 kDa and a pI of 6.0. The structure of CalB has been resolved by X-ray diffrac-

*. *Corresponding author. Mobile: +98 912 8018046; Fax: +98 87 33624133*
E-mail address: m.irani@uok.ac.ir (M. Irani)

tion [9,10]. The polypeptide chain of CalB consists of 317 amino acids, which fold into an α/β-hydrolase fold. Like other lipases, CalB is a serine hydrolase, and the active site contains a Ser-His-Asp catalytic triad. It is known that lipases function by the arrangement of catalytic triad residues in the active site. The effect of this arrangement of the residues is presumably to make the serine oxygen sufficiently nucleophilic in catalytic reactions [11-13]. The Asp residue of catalytic triad is important in catalytic activity of lipases. Theoretical studies of Brinck et al. on Serine Hydrolases revealed that removal of Asp raises the activation barrier of the ester hydrolysis reactions about 10.0 kcal/mol [13]. Experimental observations showed that replacing Asp by a neutral one increases the activation barrier by about 6 kcal/mol [14-16]. Furthermore, CalB has a limited amount of space available in the active-site pocket and thus exhibits a high degree of selectivity. Like other lipases, CalB shows a high degree of chemoselectivity, regioselectivity, and enantioselectivity. For example it shows 10^5 times higher selectivity for alcohols than for thiols in transacylation reactions [17]. It is regioselctive in reactions of rutin, isoquercitrin, and quercetinacetylation [11]. CalB enantioselctivly catalyzes the transesterification reactions of racemic 1-phenylethanol (**1-PE**) and *S*-Ethyl Thiooctanoate (**SET**) into 1-phenylethyl octanoate (Scheme 1). This transesterification reaction (the subject of this work) strongly favors the *R*-enantiomer of alcohol with an observed enantiomeric ratio greater than 200 [18].

A better understanding of the molecular foundations for the increase rate achieved by enzymes will allow us to design better catalysts for the selective enhancement of chemical transformations and to design stronger and more selective inhibitors. Scheme 1 shows the reactions of **1-PE** and **SET** catalyzed by CalB. As shown in the scheme, CalB only catalyzes the reaction of *R*-enantiomer of **1-PE** with **SET**. Our goal

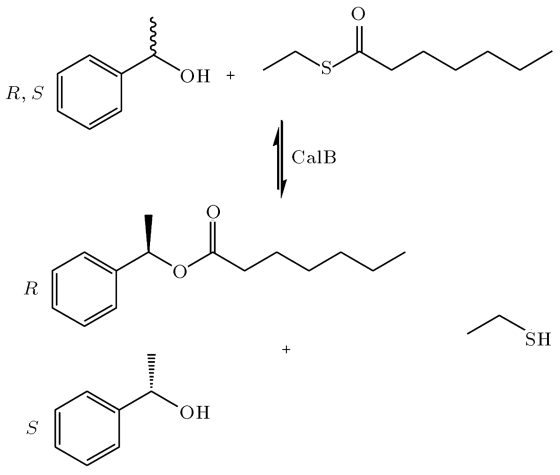

Scheme 1. Schematic view of **1-PE** and **SET** reactions catalyzed by CalB.

with this study is to increase understanding of the mechanistic aspect and enantioselectivity of CalB using DFT approaches.

Enzymes are huge molecules and it is impossible to treat a whole enzyme by Quantum Mechanics (QM). The molecular mechanics method is an alternative to treat the whole enzyme. However, this method is not appropriate to study enzymatic reactions where bonds are broken or formed. Therefore, to study the enzymatic reactions through QM methods, we have to use a model of the enzyme. The QM cluster method has been extensively used to study the catalytic mechanism and structure of enzymes [19-30]. In the QM cluster approach, a number of groups are cut out from the active site of enzyme as a model of the whole protein. It reduces the number of atoms of the protein to 50-200, which makes it possible to treat by QM or DFT methods. In order to avoid the possible significant changes in the starting crystal structure of model during geometry optimization, some atoms are kept fixed at their crystal-structure positions. In addition, the surrounding protein can provide long-range polarization that can affect the computed energies. To account for this effect, polarizable continuum techniques are usually used. These assume that the surrounding is a homogenous polarizable medium with some assumed dielectric constant. The choice of this constant is somewhat arbitrary, but ε=4 is usually considered to be a good representation of surrounding protein [31-37]. In this work, we use the crystal approach to model CalB and study its enantioselectivity and catalytic mechanism in transesterification reactions.

2. Active site models and computational methods

2.1. Active site models

To study the catalytic mechanism and enantioselectivity of CalB, two models of its active site were constructed based on the crystal structure of native enzyme (Protein Data Bank entry 1LBS) [10]. The first model (M1) consists of the catalytic triad amino acids (Asp-187, His-224 and Ser-105) and one more residue (Thr-40). The second model (M2) is bigger than M1 and consists of the amino acids of M1 and two additional residues, Gly-39 and Trp-104, as well. The amino acid residues were truncated so that only the functional groups were kept in the models (see Figure 1 for details). Following the preceding discussion in introduction, Asp-187 was modeled in its ionized form. The *R* and the *S* enantiomers of **1-PE** were constructed manually, and then each enantiomer was inserted independently into the active site, next to the catalytic triad amino acids in the models. **SET** was modeled as *S*-ethyl thiobutanote by modifying the inhibitor molecule (*n*-hexylphosphonate ethyl ester) in

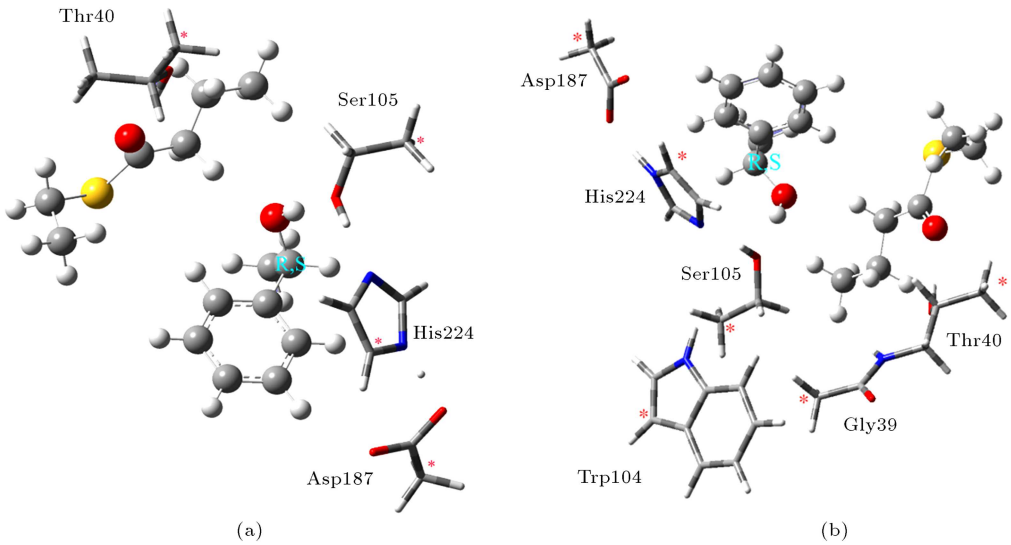

Figure 1. The optimized structures of the constructed models of the active site with the substrates (a) M1 and (b) M2. The models are shown with the *R*-enantiomer of **1-PE**. The fixed atoms are marked with asterisks. The amino acid residues are shown with tubes and the heteroatoms are shown with balls.

the crystal structure. To modify the inhibitor, we replaced the phosphor and O2P atoms (the atom names are according to their corresponding names in the PDB entry) by a carbon and a sulfur atom, respectively, and removed the propyl group from the terminal of the acyl chain (*n*-hexyl group) of inhibitor. The model of **SET** was inserted into the same place of the inhibitor, next to Thr-40. Hydrogen atoms were added manually. The total numbers of atoms are 76 and 99 in M1 and M2, respectively, and the overall charge of models is −1 because of the deprotonated Asp-187. To maintain the overall structure of active site, the carbon atoms, bound to the truncated H atoms of the active site amino acids, were fixed at their corresponding positions in the crystal structure during geometry optimizations. Figure 1 shows the optimized structures of the models with the substrates; the fixed atoms are marked with asterisks.

Thus, we have studied the reaction mechanism and enantioselectivity of CalB using the active-site models and with either the *S*- or the *R*-enantiomer of **1-PE** and the model of **SET**, as well. These models result four different states in the calculations. The reactants of these states are denoted as **M1*R*-R**, **M1*S*-R**, **M2*R*-R**, and **M2*S*-R**; **M1*R*-R** and **M1*S*-R** denote the reactant states in M1 with the *R*- or the *S*-enantiomer of **1-PE** and the model of **SET**, respectively. **M2*R*-R** and **M2*S*-R** denote the reactant states in M2 with the *R*- or the *S*-enantiomer of **1-PE** and the model of **SET**, respectively (Figure 1).

2.2. Computational methods

All calculations were performed using the density functional B3LYP [38] implemented in Gaussian 03 [39] program. Geometrical structures of the stationary points along the reaction path were optimized using 6-31+G(d) basis set. More accurate energies were then calculated from single-point calculations on the optimized structures using the 6-311++G(2d,2p) larger basis set.

The Polarized Continuum Model (PCM) is an implicit solvation model which models the solvent as a polarizable continuum, rather than individual molecules. Two types of PCMs have been popularly used: Dielectric PCM which deals with the continuum as a polarizable dielectric, and Conductor-like PCM (CPCM) which deals with the continuum as a conductor-like picture. Indeed, there is no individual solvent molecule in the model to interact with the reactants directly. To consider the surrounding protein, solvation effects were evaluated at the same level of theory of the geometry optimizations using CPCM solvation model [40,41]. We used a number of dielectric constants (ε=1, 2, 3, 4, 6, 8, 10, 20, 30, 40, 50, 60, 70, and 80) to calculate the protein medium-effect-convergence by increasing the size of the model.

Frequencies of the stationary states on the potential energy surfaces were calculated to obtain zero point energies. The frequency calculations were performed at the same level of theory of the geometry optimizations. The transition states were obtained by scanning a given distance along the reaction path as well as the structures with the highest energy along the path.

The energies discussed herein include zero-point energy and solvation energy effects.

3. Result and discussion

To propose a mechanism and to investigate enantioselectivity of the studied reaction, we have to examine

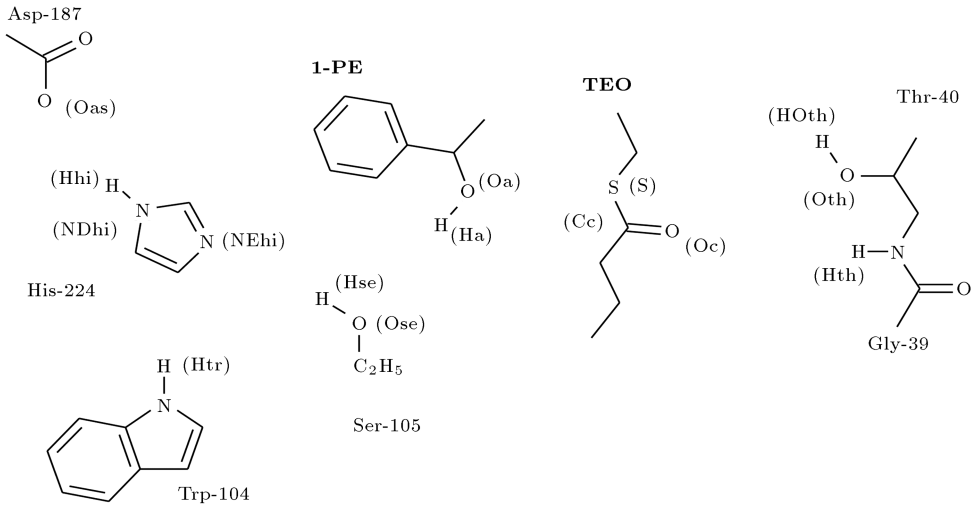

Scheme 2. Atom naming we used herein. The atom names are represented inside parentheses next to the corresponding atom.

possible paths for the reaction. We now discuss the studied paths for both *R*- and *S*-enantiomers of the alcohol with **SET**, catalyzed by CalB.

3.1. Abstraction of the alcoholic proton of 1-PE by Ser-105

We first consider abstraction of the alcoholic proton of **1-PE** (Ha) by OG of Ser-105 (Ose). (The atom names we use herein are represented in Scheme 2.) We expect the abstraction of this proton to make **1-PE** more nucleophilic than the natural alcohol. Then, the deprotonated alcohol would attack the electrophilic site of **SET** (carbonyl carbon) more conveniently. We transferred Ha in five steps, each step by shortening the Ha-Ose distance by 0.2Å. After transferring Ha to the serine residue, the hydrogen on OG of Ser-105 (Hse) transferred to NE2 of His-224 (NEhi), and the hydrogen on ND1 of the histidine (Hhi) transferred to OD1 of Asp-187 (Oas), concertedly. However, we could not find this path - the energy only increased and even after releasing the bond constraint between Ha and Ose, Ha transferred back to the alcohol. This phenomenon has happened for both *R*- and *S*-enantiomers and in both models of the enzyme. Figure 2 shows the selected structures for this path. When the bond constraint (Ha-Ose) is 1.2Å, Hse has transferred toward His-224 and Hhi has transferred toward Asp-187 (Figure 2(a)). When the bond constraint is 1.0Å, the alcoholic proton is on Ser-105, Hse is on the histidine, and Hhi is on the aspartic acid (Figure 2(b)). The optimized structure after releasing the bond constraint (Figure 2(c)) is like that in the starting point (Figure 1(a)). Therefore, we can disregard this path.

3.2. Transferring Hse to NEhi

Next, we considered another path, transferring Hse to NEhi. This proton transferring will make Ose a stronger base than a protonated alcoholic oxygen. Then, Ose can abstract the alcoholic proton of **1-PE** easier than the protonated Ose. After transferring Hse to NEhi, Hhi moves to Oas and **1-PE** moves toward Ose, concertedly. However, the energy only increases and even after releasing the bond constraint (Hse-NEhi), everything returns to the starting point, like the previous case (transferring Ha to Ose). This phenomenon has happened for both enantiomers of **1-PE** in both models of the active site. Therefore, we considered a direct path, transferring the alcohol toward the thioester.

3.3. Transferring the alcohol toward the ester

The paths of transferring Ha to Ser-105 and Hse to His-224 have not been found. In other words, the catalytic triad amino acids cannot abstract and hold the alcoholic proton, at least before nucleophilic attack of the alcohol to the ester. After rejecting the mentioned two paths, the reasonable way to perform the reaction is moving the substrates directly toward each other. We studied this path by transferring the alcohol toward the ester. The bond constraint was between Oa and Cc. We now discuss the obtained results for this path.

3.3.1. Reaction of the R-enantiomer and the thioester

The reactant states of *R*-enantiomer in M1 (**M1*R*-R**) and M2 (**M2*R*-R**) models are shown in Figure 1(a) and (b), respectively. The Oa-Cc distances are 4.12 and 4.11Å in **M1*R*-R** and **M2*R*-R**, respectively. The results show that at the structures with maximum energy (**M1*R*-TS** for M1 and **M2*R*-TS** for M2), the Cc-S distance has elongated from 1.80 to 2.06 and 1.96Å with respect to **M1*R*-R** and **M2*R*-R**, respectively. Shortening Oa-Cc and elongating Cc-S in **M1*R*-TS** and **M2*R*-TS** with respect to **M1*R*-**

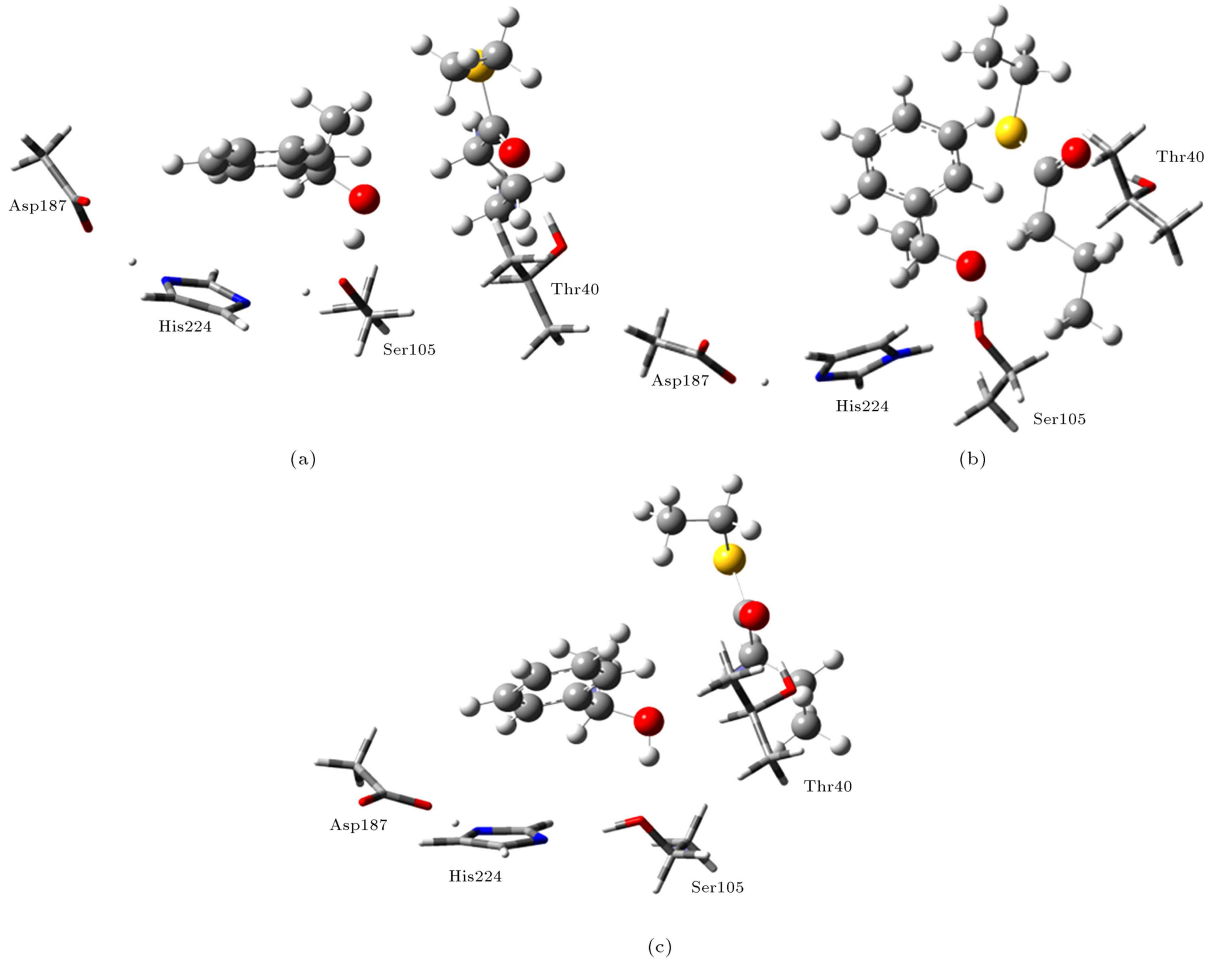

Figure 2. Selected structures in transferring the alcoholic proton of the *R*-enantiomer of **1-PE** to OG of Ser-105: (a) When Ha-Ose distance is 1.2Å; (b) when Ha-Ose distance is 1.0Å; and (c) the final sate after releasing the bond constraint.

R and **M2*R*-R** show the true reaction path. In the reaction path, by making the alcohol approach the thioester, a new ester is formed (1-phenylethyl octanoate) and the ethyl sulfide group leaves the thioester. The optimized structures along the reaction path show that by transferring the alcohol toward the thioester, Ser-105 abstracts the alcoholic proton of **1-PE**, the serine's proton moves to NEhi, and Hhi moves to Oas. These four steps has happed concertedly. On the other hand, the catalytic triad amino acids gradually increase nucleophility of the alcoholic oxygen of **1-PE** as the reaction proceeds (as the alcohol goes toward the thioester). In the product (**M1*R*-P** for M1 and **M2*R*-P** for M2), the new ester has formed and the ethyl sulfide group has drifted away from the carbonyl group (Cc-S distances are 4.35 and 5.10Åin **M1*R*-P** and **M2*R*-P**, respectively). Figure 3 shows the optimized structures of **M1*R*-TS** and **M1*R*-P**. The drifted away ethyl sulfide group can abstract a proton from the protein medium to complete its valance. The same thing has happened in the *R*-enantiomer reaction in M2. In conclusion, we can suggest a two-step mechanism for the CalB catalyzed reaction of **1-PE** and **SET**. The reaction starts by a concerted step (transferring the alcohol toward the thioester, abstracting the alcoholic proton by the catalytic triad amino acids, and drifting the ethyl sulfide group away from the thioester). After this concerted step, the new ester is formed and the ethyl sulfide group can abstract a proton from the protein medium. Then, the products can leave the active site. The selected distances for the stationary structures of *R*-enantiomer reaction and their standard deviations in the three Stationary Structures (SD) are shown in Table 1. The SDs of three distances (Ha-Oa, Oa-Cc, and Cc-S) are bigger than 1.0. These bigger SDs represent a significant change in the corresponding distances during the reaction. In other words, these three distances suffer the main changes in the reaction path due to the significant participation of them in the reaction mechanism. Scheme 3 shows our proposed mechanism for the reaction of *R*-enantiomer of the alcohol with the thioester, catalyzed by CalB.

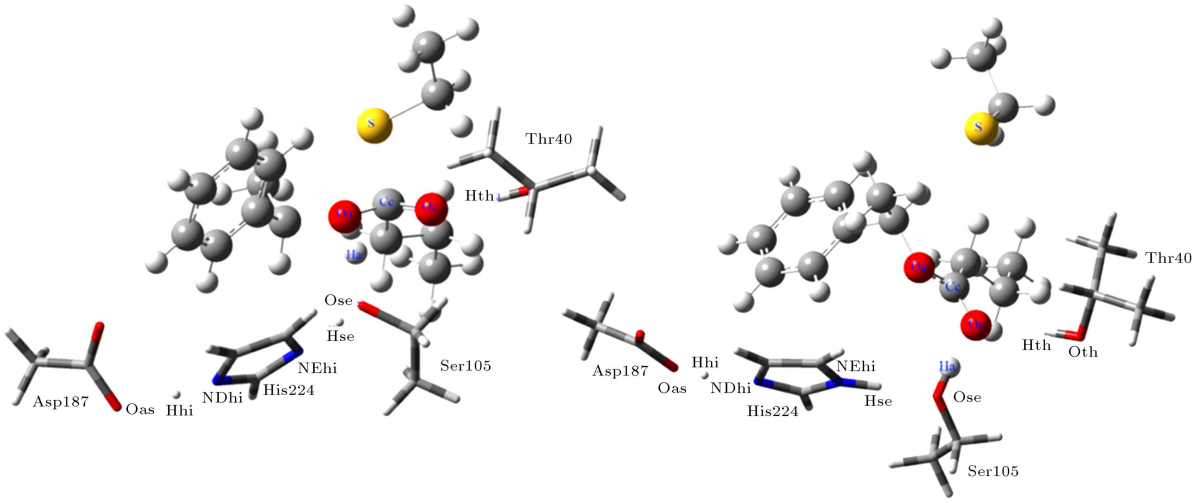

Figure 3. The structure of (a) **M1*R*-TS**, and (b) **M1*R*-P.**

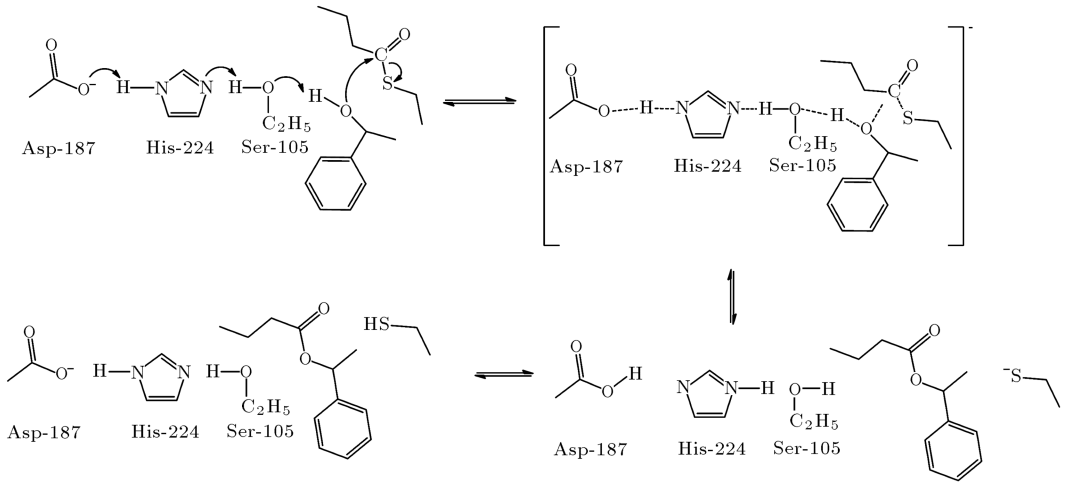

Scheme 3. The proposed mechanism for the reaction of *R*-enantiomer of the alcohol and the thioester.

Table 1. The selected distances of the stationary structures of the *R*-enantiomer reaction and their standard deviations in the three stationary structures. SDs bigger than 1.0 are shown in bold face.

	M1R-R	M1R-TS	M1R-P	SD	M2R-R	M2R-TS	M2R-P	SD
Ha-Oa	0.99	1.09	2.89	**1.07**	0.99	1.03	3.13	**1.22**
Ha-Ose	1.82	1.44	0.99	0.42	1.83	1.60	0.99	0.43
Hse-Ose	1.00	1.03	1.79	0.45	0.99	1.00	1.76	0.44
Hse-NEhi	1.77	1.66	1.03	0.40	1.84	1.77	1.04	0.44
Hhi-NDhi	1.07	1.08	1.65	0.33	1.08	1.09	1.67	0.34
Hhi-Oas	1.59	1.57	1.03	0.32	1.55	1.53	1.02	0.30
Oa-Cc	4.12	1.40	1.34	**1.59**	4.11	1.51	1.35	**1.55**
Cc-Oc	1.22	1.28	1.24	0.03	1.22	1.28	1.23	0.03
Cc-S	1.80	2.06	4.35	**1.4**	1.80	1.96	5.10	**1.86**
Htr-NEhi	–	–	–	–	1.96	2.02	2.82	0.48
HOth-Oth	0.98	0.98	0.97	0.01	0.98	0.99	1.02	0.02
Hth-Oc	–	–	–	–	4.85	3.28	4.71	0.87
Hth-Oth	–	–	–	–	2.37	2.38	2.28	0.06

3.3.2. Reaction of the S-enantiomer of the alcohol and the thioester

To study the *S*-enantiomer reaction, we performed the same distance (Oa-Cc) scanning as for the *R*-enantiomer. However, we could not find any path for the *S*-enantiomer – the energy only increased and even after releasing the bond constraint between Oa and Cc, the alcohol moved back to the reactant state. In conclusion, we can discard all paths for the *S*-enantiomer. In other words, CalB cannot catalyze the *S*-enantiomer reaction, in line with the experimental observation [18]. This result can be explained by a series of geometrical differences between the optimized structures of *R*- and *S*-enantiomers in the active site. In **M1*R*-R** and **M2*R*-R**, the alcoholic group of **1-PE** is directed toward Ose (the Ha-Ose distance is 1.82Å). In other words, there is a strong hydrogen bond between the *R*-enantiomer and Ser-105. However, the alcoholic group in the reactant state of *S*-enantiomer (**M1*S*-R** and **M2*S*-R**) is directed toward Thr-40 (see Figure 4 for an optimized structure of **M1*S*-R**) and is far from Ser-105 (the Ha-Ose distances are 5.52 and 5.00Å in **M1*S*-R** and **M2*S*-R**, respectively). The side chains of Thr-40 and Ser-105 are alcoholic functional groups. However, Thr-40 is not basic enough to abstract the alcoholic proton of **1-PE**. While, the histidine and the aspartic acid residues of the catalytic triad help Ser-105 to abstract the alcoholic proton of **1-PE** more easily. In a molecular dynamic study, Haeffner et al. [42] showed that the *R*- and *S*-enantiomers of larger and bulky alcohol substrates (3-methyl-2-butanol, and 3,3-dimethyl-2-butanol) have different hydrogen-bonding patterns in the active site of CalB. Only the hydrogen bond between the alcoholic oxygen of the substrates and the backbone of Thr-40 can be formed in two of 10 structures of *S* enantiomer of 3-methyl-2-butanol. However, this hydrogen bond cannot be formed in any of the R-enantiomers. In another molecular mechanics study, Jones et al. [10] showed that in the *R*-enantiomer, the methyl group of **1-PE** fits nicely into a small pocket in the active site. However, in the *S*-enantiomer, the methyl group is pointed toward the main chain atoms of Gly-39 and Thr-40. These make many close van der Waals contacts and these steric clashes make the *S*-enantiomer interaction highly unfavorable. However, in our results, the *R*-enantiomer reacts favorably because of its convenient hydrogen bonding with the side chain of Ser-105.

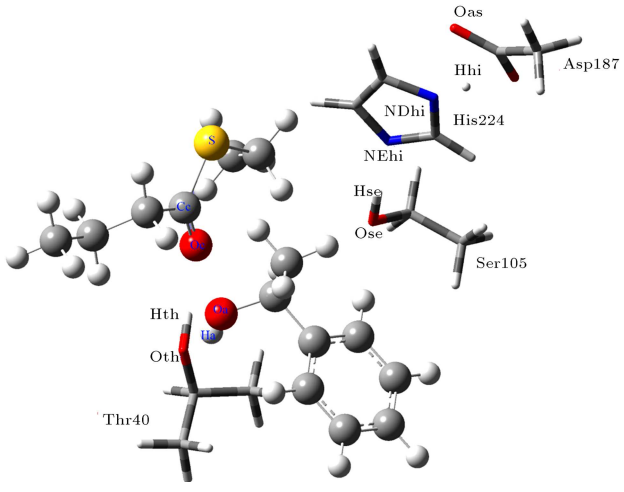

Figure 4. The optimized structure of the *S*-enantiomer of **1-PE** and **SET** in M1.

3.4. Comparison between M1 and M2 results

The two additional residues (Gly-39 and Trp-104) in M2 do not affect the reaction mechanism. However, the two models give energetically different results. The activation energy of reaction for the *R*-enantiomer is 51.3 and 43.8 kcal/mol (dielectric constant=4) in M1 and M2, respectively. The reaction energy is positive, and is 9.2 and 7.1 kcal/mol in M1 and M2, respectively. These energy differences could be related to the difference between hydrogen-bonding patterns in the models, which in turn are related to the two additional residues of M2. There is a hydrogen bond between HE1 of Trp-104 (Htr), and NEhi and there is a hydrogen bond between H (Hth) and OG1 of Thr-40 (Oth) in M2. Among these hydrogen bonds, only Hth-Oc has changed significantly from the reactant to the product (from 1.96 to 2.82Å). Elongation of this hydrogen bond could be the reason of relative destabilization of **M2*R*-P** with respect to **M1*R*-P** (greater reaction energy of M2 with respect to M1). On the other hand, the additional two residues in M2 (Gly-39 and Trp-104) do not directly participate in the reaction, but affect the energy profile of the reaction, electrostatically.

3.5. Solvation effects on the potential energy profile

The resulting energy profiles for *R*-enantiomer in various dielectric constants for the two models are shown in Figure 5. In fact, one of the important results in the last couple of years was that the solvation effects decrease very quickly with the model size. Systematic studies have shown that when the model reaches a size of 150-200 atoms, the solvation effects are saturated [22,24,43]. This observation means that at a certain model size, addition of polarizable continuum makes no difference in relative energies. Figure 5 shows the resulting energy profiles in various dielectric constants for the reaction of *R*-enantiomer. According to Figure 5, the solvation effects are saturated very quickly by increasing the model size (the effects completely vanished in M2). The energy profiles in various dielectric constants are closer to each other in M2. In conclusion, M2 is big enough to represent the protein medium electrostatic effects.

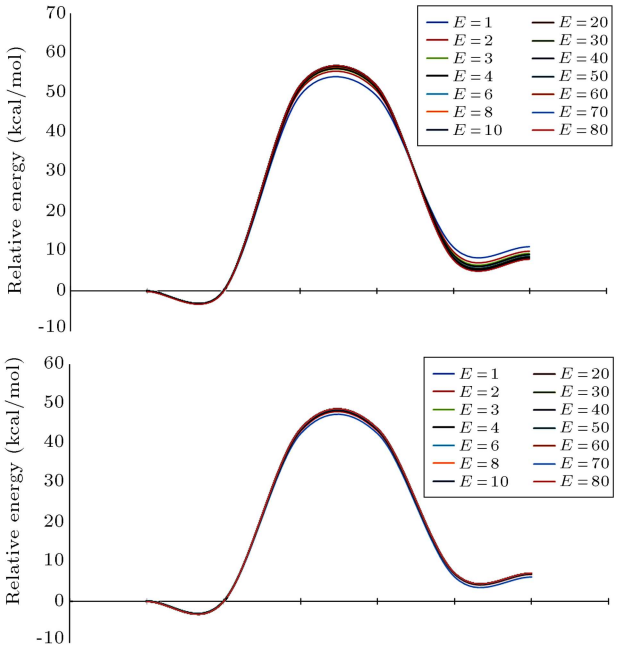

Figure 5. The resulting energy profiles in various dielectric constants for the reaction of *R*-enantiomer in (a) M1 and (b) M2.

4. Conclusion

Our results show that the catalytic triad amino acids of CalB play the key role in catalyzing the studied reaction. The amino acids do not abstract the alcoholic proton of **1-PE** before the nucleophilic attack of alcohol to the ester. The results show that there is no path for proton abstraction of the alcohol by the active site of CalB before the catalytic reaction. The reaction of *R*-enantiomer of the alcohol and the ester is a direct reaction. It is a nucleophilic attack of the alcohol to the carbonyl carbon of the ester. On the other hand, the catalytic triad amino acids gradually increase nucleophility of the alcoholic oxygen of **1-PE** as the alcohol goes toward the thioester. In other words, the catalytic triad amino acids abstract Ha by making the alcohol approach the thioester. We suggested a two-step mechanism for the CalB catalyzed reaction of *R*-enantiomer of the alcohol and the thioester. The reaction starts by a concerted step, transferring the alcohol toward the thioester, abstracting the alcoholic proton by the catalytic triad amino acids, and drifting the ethyl sulfide group away from the thioester. Then, the ester product is formed and the ethyl sulfide group abstracts a proton from the protein medium. However, we could not find any path for the *S*-enantiomer. In conclusion, we can discard all paths for the *S*-enantiomer. In other words, CalB cannot catalyze the *S*-enantiomer reaction. We proposed that the enantioselectivity of CalB is due to the different hydrogen-bonding pattern of the enantiomers of alcohol in the active site. The alcoholic proton is far from the catalytic triad amino acids in *S*-enantiomer. There is no hydrogen bond between the alcoholic hydrogen of **1-PE** and Ser-105.

Both models of the active site have the same results for the reaction mechanism. The differences are only in their predicted energy. The bigger model has less activation and bigger reaction energy than the smaller one. The energy differences could be related to the different hydrogen-bonding pattern between the two models, which in turn is related to the two additional residues of M2. The CPCM calculations showed that the solvation effects are saturated very quickly by increasing the model size. In conclusion, a model of 99 atoms (M2) is big enough to represent the protein medium electrostatic effects. The two additional groups in the bigger model do not affect the reaction mechanism. They just slightly change the energy profile or their effects are just electrostatic.

References

1. Schmid, R.D. and Verger, R. "Lipases: Interfacial enzymes with attractive applications", *Angewandte Chemie International Edition*, **37**(12), pp. 1608-1633 (1998).
2. Bornscheuer, U.T. and Kazlauskas, R.J. "Lipases and esterases", *Sections 5.3-5.4*, Wiley Online Library (1999).
3. Anderson, E.M. Larsson, K.M. and Kirk, O. "One biocatalyst-many applications: The use of *Candida antarctica* B-lipase in organic synthesis", *Biocatalysis and Biotransformation*, **16**(3), pp. 181-204 (1998).
4. Jaeger, K. Dijkstra, B. and Reetz, M. "Bacterial biocatalysts: Molecular biology, three-dimensional structures, and biotechnological applications of lipases", *Annual Reviews in Microbiology*, **53**(1), pp. 315-351 (1999).
5. Svendsen, A. "Lipase protein engineering", *Biochimica et Biophysica Acta (BBA)-Protein Structure and Molecular Enzymology*, **1543**(2), pp. 223-238 (2000).
6. Brzozowski, A., Derewenda, U., Derewenda, Z., Dodson, G., Lawson, D., Turkenburg, J., Bjorkling, F., Huge-Jensen, B., Patkar, S. and Thim, L. "A model for interfacial activation in lipases from the structure of a fungal lipase-inhibitor complex", *Nature*, **351**(6326), pp. 491-494 (1991).
7. Derewenda, U., Brzozowski, A.M. Lawson, D.M. and Derewenda, Z.S. "Catalysis at the interface: The anatomy of a conformational change in a triglyceride lipase", *Biochemistry*, **31**(5), pp. 1532-1541 (1992).
8. Zaks, A. and Klibanov, A.M. "Substrate specificity of enzymes in organic solvents vs. water is reversed", *Journal of the American Chemical Society*, **108**(10), pp. 2767-2768 (1986).
9. Uppenberg, J., Hansen, M.T., Patkar, S. and Jones, T.A. "The sequence, crystal structure determination

and refinement of two crystal forms of lipase B from *Candida antarctica*", *Structure*, **2**(4), pp. 293-308 (1994).

10. Uppenberg, J., Oehrner, N., Norin, M., Hult, K., Kleywegt, G.J., Patkar, S., Waagen, V., Anthonsen, T. and Jones, T.A. "Crystallographic and molecular-modeling studies of lipase B from *Candida antarctica* reveal a stereospecificity pocket for secondary alcohols", *Biochemistry*, **34**(51), pp. 16838-16851 (1995).

11. De Oliveira, E.B., Humeau, C., Maia, E.R., Chebil, L., Ronat, E., Monard, G., Ruiz-Lopez, M.F., Ghoul, M. and Engasser, J.-M. "An approach based on density functional theory (DFT) calculations to assess the *Candida antarctica* lipase B selectivity in rutin, isoquercitrin and quercetin acetylation", *Journal of Molecular Catalysis B: Enzymatic*, **66**(3), pp. 325-331 (2010).

12. Raza, S., Fransson, L. and Hult, K. "Enantioselectivity in Candida antarctica lipase B: a molecular dynamics study", *Protein Science*, **10**(2), pp. 329-338 (2001).

13. Hu, C.H., Brinck, T. and Hult, K. "Ab initio and density functional theory studies of the catalytic mechanism for ester hydrolysis in serine hydrolases", *International Journal of Quantum Chemistry*, **69**(1), pp. 89-103 (1998).

14. Carter, P. and Wells, J.A. "Dissecting the catalytic triad of a serine protease", *Nature*, **332**(6164), pp. 564-568 (1988).

15. Sprang, S., Standing, T., Fletterick, R., Stroud, R., Finer-Moore, J., Xuong, N., Hamlin, R., Rutter, W. and Craik, C. "The three-dimensional structure of Asn102 mutant of trypsin: Role of Asp102 in serine protease catalysis", *Science*, **237**(4817), pp. 905-909 (1987).

16. Craik, C.S., Roczniak, S., Largman, C. and Rutter, W.J. "The catalytic role of the active site aspartic acid in serine proteases", *Science*, **237**(4817), pp. 909-913 (1987).

17. Laszlo, J.A., Jackson, M. and Blanco, R.M. "Active-site titration analysis of surface influences on immobilized Candida antarctica lipase B activity", *Journal of Molecular Catalysis B: Enzymatic*, **69**(1), pp. 60-65 (2011).

18. Frykman, H., Öhrner, N., Norin, T. and Hult, K. "S-ethyl thiooctanoate as acyl donor in lipase catalysed resolution of secondary alcohols", *Tetrahedron Letters*, **34**(8), pp. 1367-1370 (1993).

19. Chen, S.-L., Fang, W.-H. and Himo, F. "Technical aspects of quantum chemical modeling of enzymatic reactions: The case of phosphotriesterase", *Theoretical Chemistry Accounts*, **120**(4-6), pp. 515-522 (2008).

20. Liao, R.-Z., Yu, J.-G. and Himo, F. "Quantum chemical modeling of enzymatic reactions: The case of decarboxylation", *Journal of Chemical Theory and Computation*, **7**(5), pp. 1494-1501 (2011).

21. Himo, F., Guo, J.-D., Rinaldo-Matthis, A. and Nordlund, P. "Reaction mechanism of deoxyribonucleotidase: A theoretical study", *The Journal of Physical Chemistry B*, **109**(42), pp. 20004-20008 (2005).

22. Georgieva, P. and Himo, F. "Quantum chemical modeling of enzymatic reactions: The case of histone lysine methyltransferase", *Journal of Computational Chemistry*, **31**(8), pp. 1707-1714 (2010).

23. Liao, R.-Z., Yu, J.-G. and Himo, F. "Tungsten-dependent formaldehyde ferredoxin oxidoreductase: Reaction mechanism from quantum chemical calculations", *Journal of Inorganic Biochemistry*, **105**(7), pp. 927-936 (2011).

24. Sevastik, R. and Himo, F. "Quantum chemical modeling of enzymatic reactions: The case of 4-oxalocrotonate tautomerase", *Bioorganic Chemistry*, **35**(6), pp. 444-457 (2007).

25. Velichkova, P. and Himo, F. "Methyl transfer in glycine N-methyltransferase. A theoretical study", *The Journal of Physical Chemistry B*, **109**(16), pp. 8216-8219 (2005).

26. Chen, S.-L., Fang, W.-H. and Himo, F. "Theoretical study of the phosphotriesterase reaction mechanism", *The Journal of Physical Chemistry B*, **111**(6), pp. 1253-1255 (2007).

27. Liao, R.-Z., Yu, J.-G., Raushel, F.M. and Himo, F. "Theoretical investigation of the reaction mechanism of the dinuclear zinc enzyme dihydroorotase", *Chemistry-A European Journal*, **14**(14), pp. 4287-4292 (2008).

28. Liao, R.-Z., Yu, J.-G. and Himo, F. "Mechanism of tungsten-dependent acetylene hydratase from quantum chemical calculations", *Proceedings of the National Academy of Sciences*, **107**(52), pp. 22523-22527 (2010).

29. Chen, S.-L., Li, Z.-S. and Fang, W.-H. "Theoretical investigation of astacin proteolysis", *Journal of Inorganic Biochemistry*, **111**, pp. 70-79 (2012).

30. Lind, M.E. and Himo, F. "Quantum chemistry as a tool in asymmetric biocatalysis: Limonene epoxide hydrolase test case", *Angewandte Chemie*, **125**(17), pp. 4661-4665 (2013).

31. Himo, F. and Siegbahn, P.E. "Quantum chemical studies of radical-containing enzymes", *Chemical Reviews*, **103**(6), pp. 2421-2456 (2003).

32. Noodleman, L. et al., "Quantum chemical studies of intermediates and reaction pathways in selected enzymes and catalytic synthetic systems", *Chemical Reviews*, **104**(2), pp. 459-508 (2004).

33. Himo, F. "C-C bond formation and cleavage in radical enzymes, a theoretical perspective", *Biochimica et Biophysica Acta (BBA)-Bioenergetics*, **1707**(1), pp. 24-33 (2005).

34. Himo, F. "Quantum chemical modeling of enzyme active sites and reaction mechanisms", *Theoretical Chemistry Accounts*, **116**(1-3), pp. 232-240 (2006).

35. Siegbahn, P.E. and Borowski, T. "Modeling enzymatic reactions involving transition metals", *Accounts of Chemical Research*, **39**(10), pp. 729-738 (2006).
36. Ramos, M.J. and Fernandes, P.A. "Computational enzymatic catalysis", *Accounts of Chemical Research*, **41**(6), pp. 689-698 (2008).
37. Siegbahn, P.E. and Himo, F. "Recent developments of the quantum chemical cluster approach for modeling enzyme reactions", *JBIC Journal of Biological Inorganic Chemistry*, **14**(5), pp. 643-651 (2009).
38. Lee, C., Yang, W. and Parr, R.G. "Development of the Colle-Salvetti correlation-energy formula into a functional of the electron density", *Physical Review B*, **37**(2), pp. 785-789 (1988).
39. Frisch, M.J., Trucks, G.W., Schlegel, H.B., et al. *Gaussian 03, Revision C.02* (2003).
40. Barone, V. and Cossi, M. "Quantum calculation of molecular energies and energy gradients in solution by a conductor solvent model", *The Journal of Physical Chemistry A*, **102**(11), pp. 1995-2001 (1998).
41. Cossi, M., Rega, N., Scalmani, G. and Barone, V. "Energies, structures, and electronic properties of molecules in solution with the C-PCM solvation model", *Journal of Computational Chemistry*, **24**(6), pp. 669-681 (2003).
42. Haeffner, F., Norin, T. and Hult, K. "Molecular modeling of the enantioselectivity in lipase-catalyzed transesterification reactions", *Biophysical Journal*, **74**(3), pp. 1251-1262 (1998).
43. Hopmann, K.H. and Himo, F. "Quantum chemical modeling of the dehalogenation reaction of haloalcohol dehalogenase", *Journal of Chemical Theory and Computation*, **4**(7), pp. 1129-1137 (2008).

Biographies

Mehdi Irani was born in Tabriz, Iran, in 1982. He received a BS degree in Chemistry from the University of Kurdistan, Sanandaj, Iran, in 2004, and MS and PhD degrees in Physical Chemistry from Sharif University of Technology, Tehran, Iran, in 2006 and 2010, respectively. He has been a faculty member at Chemistry Department in the University of Kurdistan, Sanandaj, Iran, since 2011. His main research interests include quantum chemistry and computational biochemistry.

Saied Heydaryan was born in Kermanshah, Iran, in 1984. He received his BS degree in Chemistry from Payame Noor University, Kermanshah, Iran, in 2008, and his MS degree in Physical Chemistry from the University of Kurdistan, Sanandaj, Iran, in 2014, under supervision of Dr. Irani. His research interests include quantum chemistry and computational biochemistry.